

13. An adjusted array hybridization intensity value ( $I$ ) was determined for each hybridization (20 altogether) as the mean of the  $\log(\text{PM})$  signals of all features that showed minimal variation across all hybridizations (the nonmarkers, determined recursively as described below). Then, for each feature on the array, a linear regression of  $\log(\text{perfect match (PM)})$  on  $I$  for all hybridizations was determined by the least squares method, first under the null hypothesis that the S96 and YJM789 samples had the same response and then under the alternative hypothesis that the S96 samples had a greater signal than the YJM789 samples. The models were compared with the  $F$  test, and the same signal model was rejected in favor of a marker with 99% confidence. This software is available upon request to D. Richards.
14. Gaps were often found near regions with low probe coverage, for example, near repeated elements in the genome or regions of low open reading frame (ORF) density. However, in some cases, probe coverage was adequate, suggesting that the gap might be due to a high amount of sequence conservation or to the region having a recent common origin for the two strains.
15. The  $p$  is computed as  $P(S96)/[P(S96)+P(YJM789)]$ , where  $P(X)$  is the probability (from the  $t$  distribution) that a marker has genotype  $X$ , based on the observed (PM) hybridization signal of the feature and the expected signal (given the array hybridization intensity) and the estimated variance from the regression for the marker.
16. J. M. Cherry *et al.*, *Nature* **387**, 67 (1997).
17. T. Petes, R. Malone, L. Symington, in *The Molecular and Cellular Biology of the Yeast Saccharomyces*, J. Broach, J. Pringle, E. Jones, Eds. (Cold Spring Harbor Laboratory, Cold Spring Harbor, NY, 1991), vol. 1, pp. 407–521.
18. B. Chattoo *et al.*, *Genetics* **93**, 51 (1979).
19. E. Alani, L. Cao, N. Kleckner, *ibid.* **116**, 541 (1987).
20. Yeast strains were routinely grown in yeast extract, peptone, and dextrose (YEPD) medium; sporulation medium and defined medium for scoring auxotrophs were prepared as previously described [F. Sherman, G. Fink, C. Lawrence, *Methods in Yeast Genetics: Laboratory Manual* (Cold Spring Harbor Laboratory, Cold Spring Harbor, NY, 1974)]. Segregants were complementation tested to distinguish *lys2* from *lys5*. Cycloheximide sensitivity was scored by inability to grow on YEPD plates containing cycloheximide (0.5  $\mu\text{g/ml}$ ). All segregants from the 99 tetrads were phenotyped for *lys2*, *lys5*, and *cyh*. *lys5* and *cyh* segregated 2:2 for 99 tetrads, and *lys2* segregated 2:2 for 98 of the 99. Selected segregants were scored for *MAT* and *ho*. The *ho* and *ho::hisG* were distinguished by checking the size of PCR products on a gel, and *MAT* was determined by mating and complementation.
21. The loci could have been mapped with any segregant as long as the genotype was known; however, segregants with similar genotypes were chosen to simplify the analysis.
22. The probability of an interval segregating 10 to 0 randomly (a false positive) was estimated to be about 40% for each outcome. No false positives were observed with 10 segregants, and therefore no additional hybridizations were performed. This conservative estimate of probability, which does not take into account recombination hotspots or interference, was calculated by dividing the genome size (12 Mb) by the average interval (29 kb for 10 segregants with 1 cM = 2.9 kb for yeast) and then multiplying this number by the probability of 10 events having the same outcome  $(1/2)^N$ . In general, up to 13 segregants (or more if the trait is non-Mendelian) may need to be examined to have a 95% probability of identifying a single region as responsible for a trait.
23. The breakpoints were recursively added to each chromosome on the basis of the  $p$  values. The probabilities of breakpoints at every pair of markers were tested against the probability of no breakpoint. The breakpoints that maximized this likelihood were accepted if the logarithmic likelihood ratio was greater than 30.
- This procedure was repeated for each new subinterval created by a breakpoint to 500-bp resolution.
24. M. Boehnke, *Am. J. Hum. Genet.* **55**, 379 (1994).
25. E. Balzi, M. Wang, S. Leterme, L. Van Dyck, A. Goffeau, *J. Biol. Chem.* **269**, 2206 (1994).
26. E. A. Winzeler *et al.*, unpublished data.
27. J. H. McCusker, K. V. Clemons, D. A. Stevens, R. W. Davis, *Genetics* **136**, 1261 (1994).
28. D. G. Wang *et al.*, *Science* **280**, 1077 (1998).
29. P. A. Underhill *et al.*, *Genome Res.* **7**, 996 (1997).
30. M. Orita, H. Iwahana, H. Kanazawa, K. Hayashi, T. Sekiya, *Proc. Natl. Acad. Sci. U.S.A.* **86**, 2766 (1989).
31. D. J. Lockhart *et al.*, *Nature Biotechnol.* **14**, 1675 (1996).
32. We thank N. Risch and D. Siegmund for helpful advice. E.A.W. is supported by the John Wasmuth Fellowship in Genomic Analysis (HG00185-01). D.R.R. is a Howard Hughes Medical Institute predoctoral fellow. M.J.M. is supported by a Commonwealth AIDS Research Grants Committee of Australia postdoctoral overseas fellowship. Funding by NIH grant 1R01 HG01633.

28 January 1998; accepted 21 July 1998

## Prototype of a Heme Chaperone Essential for Cytochrome c Maturation

Henk Schulz, Hauke Hennecke, Linda Thöny-Meyer\*

Heme, the iron-containing cofactor essential for the activity of many enzymes, is incorporated into its target proteins by unknown mechanisms. Here, an *Escherichia coli* hemoprotein, CcmE, was shown to bind heme in the bacterial periplasm by way of a single covalent bond to a histidine. The heme was then released and delivered to apocytochrome c. Thus, CcmE can be viewed as a heme chaperone guiding heme to its appropriate biological partner and preventing illegitimate complex formation.

In c-type cytochromes, heme is bound covalently by way of two thioether bonds to the conserved CXXCH motif of the apoprotein in a posttranslational process referred to as cytochrome c maturation (1–3). Heme synthesis in the mitochondrial matrix (4) or bacterial cytoplasm (2), and the stereospecific, covalent heme attachment in the intermembrane space (3) or periplasm (5, 6) are spatially separated processes requiring heme trafficking. Heme addition in mitochondria has been attributed to the enzyme cytochrome c heme lyase (3, 7), although neither the mode of heme binding to that enzyme nor the mechanism of the ligation reaction has been elucidated. In *Escherichia coli*, eight *ccm* genes encode membrane proteins that are essential for cytochrome c maturation (8, 9).

*Escherichia coli* genes *ccmABCDEFGH* were overexpressed from a plasmid to stimulate cytochrome c maturation. Analysis of the membrane fraction by SDS–polyacrylamide gel electrophoresis (SDS–PAGE) revealed an 18-kD protein that retained peroxidase activity of c-type cytochromes with covalently bound heme. However, the size of this protein corresponded best to one of the products of the *ccm* genes, CcmE. A chromosomal in-frame deletion mutant, which was constructed by removing 92 *ccmE*-internal

codons (Ile<sup>3</sup> to Ser<sup>94</sup>) (10), was unable to produce mature c-type cytochromes (Fig. 1A). When *ccmE* was expressed in the  $\Delta\text{ccmE}$  background from the arabinose-inducible promoter  $p_{\text{ara}}$  (11), membranes of the complementing strain contained both endogenous holocytochromes c and high levels of proposed heme-binding CcmE (Fig. 1A), as confirmed by immunoblot (Fig. 1B). The heme-protein association was SDS-resistant, as demonstrated by labeling *ccmE*-expressing *E. coli* cells with the heme precursor [<sup>14</sup>C]- $\delta$ -aminolevulinic acid ( $\delta$ -ALA) followed by SDS–PAGE of trichloroacetic acid (TCA)-precipitated cell extracts (12). Cells expressing the eight *ccm* genes plus the two naturally adjacent structural genes for the endogenous c-type cytochromes NapB and NapC on a multicopy plasmid (6) were transformed with a second plasmid containing an additional, arabinose-inducible *ccmE* gene and analyzed for heme-binding proteins (Fig. 1C). When *ccmE* expression from  $p_{\text{ara}}$  was repressed by the addition of glucose, endogenous *E. coli* c-type cytochromes such as NapB and NapC and the 18-kD CcmE protein were labeled to a similar extent. When *ccmE* was overexpressed by arabinose induction, however, most of the [<sup>14</sup>C] label was incorporated into the 18-kD protein, confirming that CcmE contains a covalently bound tetrapyrrole. We conclude that the peroxidase activity (Fig. 1A) resulted from the presence of bound heme.

Next we characterized the spectroscopic features of the 18-kD hemoprotein. A hexa-

Mikrobiologisches Institut, Eidgenössische Technische Hochschule, Schmelzbergstrasse 7, CH-8092 Zürich, Switzerland.

\*To whom correspondence should be addressed. E-mail: lthoeny@micro.biol.ethz.ch

## REPORTS

histidine tag ( $H_6$ ) was fused to the  $NH_2$ -terminus of CcmE. The protein was overexpressed in a  $\Delta ccmE$  background and purified from membranes (13). Pure CcmE- $H_6$  protein migrated as a prominent 20-kD heme-staining band (Fig. 1, A and B). Visual light spectroscopy of dithionite-reduced and ammonium persulfate-oxidized CcmE- $H_6$  protein was performed and the difference spectrum recorded (Fig. 2A). Maxima of  $\alpha$ ,  $\beta$ , and  $\gamma$  peaks were detected at 554.5, 524.5, and 426.5 nm, respectively, which is characteristic of c-type cytochromes (14). The pyridine hemochrome spectrum (14) showed peaks at 550.5, 520, and 420.5 nm, again typical for covalently bound heme. A stoichiometry of one molecule heme per three molecules CcmE polypeptide was calculated. This suggested that possibly not every CcmE molecule was charged with heme. After classical heme extraction with acidic acetone (14), no heme was detected in the organic solvent. Neither boiling of the protein for 30 min in 2% SDS and 6 M urea, nor overnight treatment with 50 mM  $HgCl_2$ -6 M urea (pH 2) removed heme from the polypeptide. Thus, heme appeared to be bound covalently to the CcmE polypeptide.

In order to overproduce CcmE in its natural cellular compartment, we first examined its topology by CcmE-PhoA fusion analysis (15). Alkaline phosphatase lacking its own signal sequence was fused to the last amino acid of CcmE. PhoA activity was expected only if CcmE was able to translocate the fused PhoA reporter to the periplasm. Cells containing the CcmE<sub>159</sub>-PhoA fusion plasmid produced  $216.2 \pm 0.4$  phosphatase units, compared with 0.6 units of control cells containing the same plasmid lacking the *phoA* coding sequence. Thus, CcmE was anchored in the membrane by a hydrophobic,  $NH_2$ -terminal domain and its

bulk was oriented toward the periplasm.

A soluble,  $H_6$ -tagged CcmE was produced as both a cytoplasmic (c-CcmE- $H_6$ ) and a periplasmic (p-CcmE- $H_6$ ) protein (Fig. 1B) (16) and tested for heme binding (Fig. 1A). Only the periplasmic version was heme stainable, suggesting that heme binding occurs in the periplasm.

The soluble p-CcmE- $H_6$  protein was purified (13), then digested with trypsin, and a heme-binding peptide with an  $\alpha$  absorption peak at 554 nm was isolated (17). Edman

degradation resulted in the amino acid sequence XDENYTPPEVEZ (18) that matched the tryptic peptide HDENYTPPEVEK, except at the first position (X), where an extremely hydrophobic, nonidentifiable residue was found, and at the last position (Z), which is not conserved in the known CcmE homologs (2) and, therefore, is not likely the heme-binding residue. To unambiguously characterize the heme-bound tryptic peptide, we performed ion spray mass spectrometry (19) and obtained a molecular weight of 2073. This corresponded well to the sum of the theoretical molecular weights of the HDENYTPPEVEK peptide (1457.65) plus heme (616.55). Tandem mass spectrometry (MS/MS) of the parent ion [mass-to-charge ratio ( $m/z$ ) = 1038;  $z = 2$ ] resulted in two dominant daughter ions with molecular weights of 617 and 1459 corresponding to heme and the tryptic peptide, respectively (Fig. 2B). Various minor daughter ions were also obtained, among them ions with molecular weights of 1112, 1275, and 1377 corresponding to heme-HDEN, heme-HDENY, and heme-HDENYT, respectively. This result implied that heme was bound to one of the first four amino acids of the tryptic peptide. Consistent with the Edman degradation data we inferred that His<sup>130</sup> of CcmE is the residue that is derivatized with covalently bound heme. To confirm this, we changed His<sup>130</sup> to alanine by site-directed mutagenesis. The mutated CcmE protein was produced in the  $\Delta ccmE$  strain and tested for heme binding. As expected, only apo-CcmE was detected, and cytochrome c maturation was not restored. Therefore, His<sup>130</sup> is essential for both heme binding and cytochrome c maturation. It resides near the center of a seven-amino acid stretch (VLAKHDE) that is strictly conserved in all CcmE-like proteins (2) and

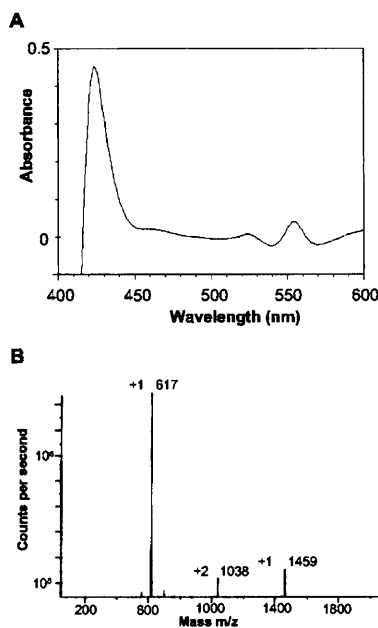
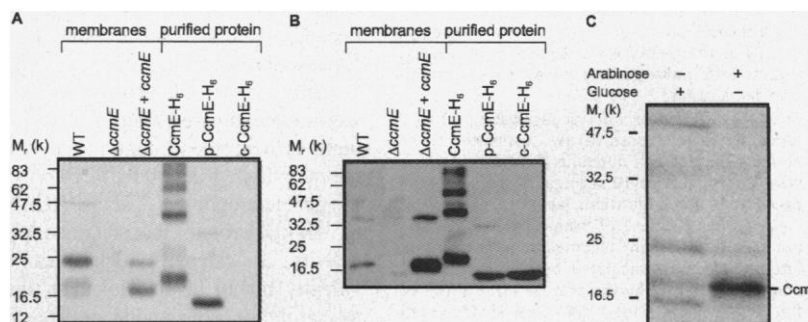


**Fig. 2.** Spectroscopic characterization of CcmE. (A) Dithionite-reduced minus ammonium persulfate-oxidized difference spectrum of purified,  $H_6$ -tagged CcmE ( $0.6 \text{ mg ml}^{-1}$ ). (B) Tandem mass spectrum of the parent ion ( $m/z = 1038$ ;  $z = 2$ ) from the tryptic CcmE heme peptide. The recorded masses are indicated on the right, the charges on the left of the peaks.

**Fig. 1.** Identification of CcmE as a heme-binding protein. (A) Heme stain of proteins separated by 15% SDS-PAGE. For membrane fractions, we applied (from left to right) 150, 150, and 50  $\mu\text{g}$  of membrane proteins from cells grown anaerobically in the presence of 5 mM nitrite for expression of endogenous c-type cytochromes: wild-type (WT) cointegrate (*ccmABCDEFHG*<sup>+</sup>),  $\Delta ccmE$  mutant cointegrate, and  $\Delta ccmE$  mutant cointegrate complemented with *ccmE* overexpressed on a plasmid. The endogenous c-type cytochromes of 18 and 24 kD are most likely the NrfB and NapC proteins, respectively (9). Wild-type CcmE migrates slightly faster than NrfB. For purified proteins, 8, 10, and 10  $\mu\text{g}$  of purified, histidine-tagged CcmE derivatives were loaded. Membrane-bound CcmE- $H_6$  migrates at  $\sim 20$  kD; the soluble,  $H_6$ -tagged periplasmic (p-CcmE- $H_6$ ) and cytoplasmic (c-CcmE- $H_6$ ) versions of CcmE have apparent molecular masses of 15 kD. Molecular size standards are indicated on the left. (B) Protein immunoblot of a gel similar to that in (A) developed with anti-CcmE (77, 23). For membrane fractions, lanes were loaded with (from left to right) 20, 20, and 3  $\mu\text{g}$  of protein, and for purified proteins, 1, 10, and 10  $\mu\text{g}$ . Migration of heme-charged p-CcmE- $H_6$  and heme-free c-CcmE- $H_6$  was indistinguishable in the gel. (C) Radiolabeling of CcmE with the heme precursor [<sup>14</sup>C]- $\delta$ -ALA. The  $\Delta ccmA-H$  strain ECO6 was complemented with plasmid pEC66 carrying the *napBCcmABCDEFHG* genes (6, 8) plus



an arabinose-inducible *ccmE* gene on a second plasmid. Whole cells labeled with 42.9  $\mu\text{M}$  [<sup>14</sup>C]- $\delta$ -ALA for 1 hour (12) in the presence of either glucose or arabinose (repressing or inducing *ccmE* expression from *p<sub>ara</sub>*, respectively) were precipitated with TCA, and proteins were separated by 15% SDS-PAGE. Radiolabeled proteins were visualized on a PhosphorImager. Expression of the *ccm* genes from pEC66 resulted in four major labeled bands corresponding to the NrfA (50 kD), NapC (24 kD), NrfB/CcmE (18 kD), and NapB (16 kD) c-type cytochromes (9). Upon addition of 0.8% arabinose, cells overexpressed CcmE into which most of the radiolabel was incorporated.

## REPORTS

may thus represent a previously undescribed heme-binding motif.

Does the cytochrome *c* maturation pathway in *E. coli* involve a step where CcmE binds heme tightly and transfers it subsequently to the apocytochrome *c*? An *E. coli* strain was constructed that expressed *ccmE* constitutively from a plasmid carrying all of the *ccm* genes downstream of a *tet* promoter. In addition, the *Bradyrhizobium japonicum* *cyoA* gene encoding the soluble *B. japonicum* cytochrome *c*<sub>550</sub> was expressed from the inducible *p<sub>ara</sub>* promoter (20). Figure 3A shows the kinetics of holo-CcmE and holo-cytochrome *c*<sub>550</sub> formation upon induction of apocytochrome *c*<sub>550</sub> expression. Although CcmE contained heme by the time of induction, the signal intensity decreased with time. Holo-cytochrome *c*<sub>550</sub> appeared 2 to 3 min after induction and accumulated at later time points. Immunoblotting of parallel samples demonstrated that they all contained constant amounts of CcmE polypeptide throughout the experiment (Fig. 3B). When expression of a heme-binding site mutant apocytochrome *c* (CLASH instead of the wild-type CLACH) (20) was induced in the presence of CcmE, heme remained bound to CcmE, which indicated that only wild-type apocytochrome *c* was able to trigger the release of heme from CcmE (Fig. 3C, upper and middle panels). Likewise, release of heme from CcmE was blocked in the absence of the CcmFGH proteins (Fig. 3C, lower panel), indicating that transfer of heme from CcmE to apocytochrome *c* re-

quires at least one of these proteins.

CcmE represents a prototype of hemo-protein that binds heme covalently by a single bond to a histidine. Our MS data suggest that this binding does not involve a major loss of atoms from either the porphyrin or the histidine, which is likely due to an addition of the histidine imidazole to the double bond of one of the vinyl side chains of heme. The chemical nature of the bond may have implications for the precise mechanism of heme attachment to apocytochrome *c*.

CcmE appears to capture heme in the periplasm and promote transfer to newly synthesized apocytochrome *c*. The binding of heme to CcmE is a prerequisite for the subsequent heme ligation. CcmE may serve as periplasmic heme chaperone by (i) preventing heme from precipitation, (ii) hindering its nonspecific association with the membrane owing to its high hydrophobicity, (iii) presenting it in a sterically suitable conformation to the apocytochrome, or (iv) activating it for subsequent attachment to apocytochrome.

A *ccmE* gene has so far been identified only in representatives of the  $\alpha$  and  $\gamma$  subdivisions of proteobacteria (2) and in the *Arabidopsis* plant (21). Other cytochrome *c*-forming organisms (for example, yeast, *Bacillus subtilis*, *Helicobacter pylori*, *Synechocystis* sp., *Archaeoglobus fulgidus*) seem to use a *ccm*-independent mechanism (22). Perhaps distinct types of heme chaperones will be identified in alternative cytochrome *c* maturation pathways.

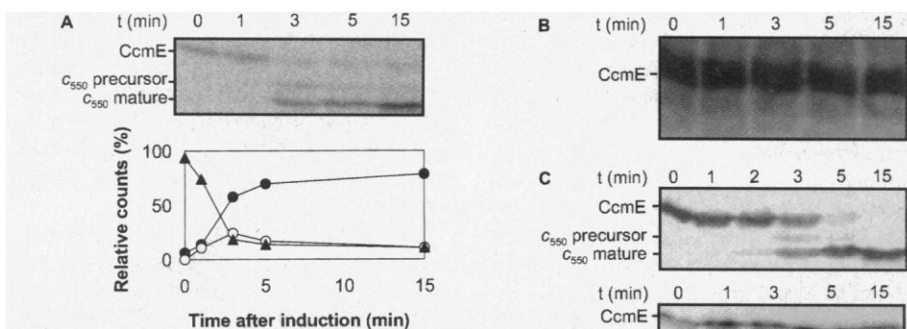


**Fig. 3.** Heme transfer from CcmE to apocytochrome *c*. (A) [<sup>14</sup>C]- $\delta$ -ALA-labeled cells (12) expressing *ccmE* constitutively were induced for expression of the *B. japonicum* apocytochrome *c*<sub>550</sub>. Samples (0.5 ml) were precipitated with TCA. Proteins were separated by 15% SDS-PAGE and visualized after 2 weeks of exposure on a PhosphorImager. The faint band migrating above holo-cytochrome *c* represents most likely the uncleaved, heme-binding precursor-cytochrome *c*, supporting the finding that cleavage of the signal sequence from the precursor is not obligate before heme attachment (6). The signal intensities were quantified by equalizing them such that the counts of each lane added up to 100%. ( $\blacktriangle$ ) CcmE, ( $\circ$ ) unprocessed cytochrome *c*<sub>550</sub> precursor, and ( $\bullet$ ) mature cytochrome *c*<sub>550</sub>. (B) Immunoblot of a gel similar to that in (A) developed with anti-CcmE immunoglobulins. (C) Heme stains of TCA-precipitated samples prepared as in (A) except that cells were not labeled. (Top) Induction was performed in the presence of all *ccm* genes. (Middle) A heme-binding site mutant (20) of cytochrome *c*<sub>550</sub> was expressed. (Bottom) Wild-type apocytochrome *c*<sub>550</sub> was expressed in the presence of *ccmABCDE*, but in the absence of *ccmFGH* (24).

## References and Notes

1. L. Thöny-Meyer, D. Ritz, H. Hennecke, *Mol. Microbiol.* **12**, 1 (1994); G. Howe and S. Merchant, *Photosynth. Res.* **40**, 147 (1994); M. D. Page et al., *Trends Biochem. Sci.* **23**, 103 (1998); R. G. Kranz et al., *Mol. Microbiol.* **29**, 383 (1998).
2. L. Thöny-Meyer, *Microbiol. Mol. Biol. Rev.* **61**, 337 (1997).
3. D. H. Gonzales and W. Neupert, *J. Bioenerg. Biomembr.* **22**, 753 (1990).
4. H. A. Dailey, in *Biosynthesis of Heme and Chlorophylls* (McGraw-Hill, New York, 1990), pp. 123–160.
5. Y. Sambongi, R. Stoll, S. J. Ferguson, *Mol. Microbiol.* **19**, 1193 (1996).
6. L. Thöny-Meyer and P. Künzler, *Eur. J. Biochem.* **246**, 794 (1997).
7. G. Basile, C. Di Bello, H. Taniuchi, *J. Biol. Chem.* **255**, 7181 (1980); B. Hennig and W. Neupert, *Eur. J. Biochem.* **121**, 203 (1981).
8. L. Thöny-Meyer et al., *J. Bacteriol.* **177**, 4321 (1995).
9. J. Grove et al., *Mol. Microbiol.* **19**, 467 (1996).
10. *Escherichia coli* K-12 strains used for *ccmE* expression and cytochrome *c* analysis are derivatives of MC1061 [P. S. Meissner, W. P. Sisk, M. L. Bergman, *Proc. Natl. Acad. Sci. U.S.A.* **84**, 4171 (1987)]. The chromosomal  $\Delta$ *ccmE* deletion of 92 codons (le<sup>3</sup> to Ser<sup>94</sup>) was constructed by polymerase chain reaction (PCR)-based cloning and subsequent gene replacement mutagenesis of the wild-type strain MC1061. A pMAK705-derived plasmid with a temperature-sensitive origin of replication [C. M. Hamilton et al., *J. Bacteriol.* **171**, 4617 (1989)] containing the *ccmA* gene expressed constitutively from the pACYC184-derived *tet* promoter [A. C. Y. Chang and S. N. Cohen, *ibid.* **134**, 1141 (1978)] was co-integrated into the wild type at high temperatures to obtain enhanced and anaerobiosis-independent expression of the *ccm* genes, which stimulated holo-cytochrome *c* formation. An equivalent strain carrying the  $\Delta$ *ccmE* mutation ( $\Delta$ *ccmE* co-integrate) was obtained by co-integrating the same plasmid into the chromosomal  $\Delta$ *ccmE* mutant. The  $\Delta$ *ccmE* co-integrate was used as a background for expression of the various CcmE proteins described in this work.
11. The vector for *ccmE* overexpression was pISC3, a pISC2 (17) derivative with an Xba I site replacing the unique Nde I site of pISC2 downstream of the *p<sub>ara</sub>* promoter. The plasmid has a ColE1 origin of replication and contains the *araC* gene encoding the activator protein that induces transcription at *p<sub>ara</sub>* in the presence of arabinose.
12. Labeling of cells with [<sup>14</sup>C]- $\delta$ -ALA was performed with exponentially growing cells [absorbance at 578 nm (*A*<sub>578</sub>) = 0.6] in LB medium, to which 42  $\mu$ M [<sup>14</sup>C]- $\delta$ -aminolevulinic acid (1.762 GBq/mmol, NEN) was added. After 1 hour, proteins were precipitated with TCA and applied to 15% SDS-PAGE. Radioactively labeled hemoproteins were detected on a PhosphorImager SF (Molecular Dynamics).
13. H<sub>6</sub>-tagged protein was isolated in the presence (for CcmE from membranes solubilized in 2% Triton X-100) or absence (for soluble CcmE) of 0.1% Triton X-100 by Ni<sup>2+</sup> affinity chromatography on nitrilotriacetic acid (NTA) agarose (Quiagen).
14. J.-H. Fuhrhop and K. M. Smith, in *Porphyrins*, K. M. Smith, Ed. (Elsevier, Amsterdam, 1975), pp. 757–868. Heme was quantified with an extinction coefficient at 551 nm ( $\epsilon$ <sub>551</sub>) = 29.1 mM<sup>-1</sup> cm<sup>-1</sup> in the pyridine hemochrome assay. CcmE polypeptide concentration was quantified after S. C. Gill and H. P. van Hippel [*Anal. Biochem.* **182**, 319 (1989)].
15. C. Manoil and J. Beckwith, *Science* **233**, 1403 (1986).
16. Cytoplasmic CcmE-H<sub>6</sub> was produced from a construct in which an ATG start codon was fused to the coding sequence for the COOH-terminal 130 amino acids of CcmE (Leu<sup>30</sup> to Ser<sup>159</sup>) plus six histidines. For the periplasmic version, the cleavable *E. coli* OmpA signal sequence was fused to that sequence. The fused genes were placed under the control of the *p<sub>ara</sub>* promoter for overproduction. Both CcmE versions were expressed in a  $\Delta$ *ccmE* background upon induction with arabinose.
17. p-CcmE-H<sub>6</sub> was digested with trypsin (1% w/w) at

- 37°C for 5 hours, and the peptides were separated on a LiChrospher RP-8 HPLC-Cartridge (Hewlett-Packard) with a linear acetonitrile gradient in 0.1% (v/v) TFA. Peptides were monitored at 215 and 415 nm to detect the heme-binding peptide. The peak fraction was collected, lyophilized, and resuspended in 50% (v/v) acetonitrile, 0.1% (v/v) acetate.
18. Abbreviations for the amino acid residues are as follows: A, Ala; C, Cys; D, Asp; E, Glu; F, Phe; G, Gly; H, His; I, Ile; K, Lys; L, Leu; M, Met; N, Asn; P, Pro; Q, Gln; R, Arg; S, Ser; T, Thr; V, Val; W, Trp; and Y, Tyr.
  19. MS/MS analysis was performed with a micro-ion-spray ion source on a API 365 LC/MS/MS system (Perkin-Elmer) with a flow rate of 15  $\mu$ l per hour. The first and third quadrupole were set to scan the mass range of 500 to 2500 *m/z*. The collision gas in the second quadrupole was nitrogen.
  20. L. Thöny-Meyer, P. Künzler, H. Hennecke, *Eur. J. Biochem.* **235**, 754 (1996).
  21. F. Grellet *et al.*, GenBank accession number U72502 (1996).
  22. B. S. Goldman and R. G. Kranz, *Mol. Microbiol.* **27**, 871 (1998).
  23. Preparation of membranes, soluble fractions, and the periplasmic fraction and determination of protein concentration, SDS-PAGE, heme staining, protein immunoblot analysis, and visual light spectroscopy were performed as described [L. Thöny-Meyer, D. Stax, H. Hennecke, *Cell* **57**, 683 (1989); R. A. Fabianek, H. Hennecke, L. Thöny-Meyer, *J. Bacteriol.* **180**, 1947 (1998); R.

- Zufferey *et al.*, *J. Biol. Chem.* **273**, 6452 (1998)]. CcmE-specific antiserum directed against the synthetic peptide K<sup>129</sup>HDENYTPPEKAME<sup>144</sup> was purchased from TANA Laboratories (Houston, TX).
24. The *ccmABCDE* genes were expressed constitutively from the pACYC184-derived tet promoter in a  $\Delta$ *ccm-ABCDEF* background (8).
  25. We thank H. Troxler (Department of Pediatrics, University of Zürich) for mass spectrometry analysis, W. Staudenmann and P. James for protein sequence analysis, A. Hungerbühler for technical assistance, and M. Aebi and A. Helenius for constructive comments on the manuscript. Supported by a grant from the Swiss National Foundation for Scientific Research.
- 21 April 1998; accepted 1 July 1998

## Determinants of Kinesin Motor Polarity

Sharyn A. Endow\* and Kimberly W. Waligora

The kinesin motor protein family members move along microtubules with characteristic polarity. Chimeric motors containing the stalk and neck of the minus-end-directed motor, Ncd, fused to the motor domain of plus-end-directed kinesin were analyzed. The Ncd stalk and neck reversed kinesin motor polarity, but mutation of the Ncd neck reverted the chimeric motor to plus-end movement. Thus, residues or regions contributing to motor polarity must be present in both the Ncd neck and the kinesin motor core. The neck-motor junction was critical for Ncd minus-end movement; attachment of the neck to the stalk may also play a role.

Most kinesins (1) move toward the unstable plus ends of their filamentous tracks, the microtubules, but some move toward the more stable minus ends. What is the molecular basis of directionality of plus- and minus-end kinesin movement? Chimeric motor proteins consisting of the Ncd motor domain, the region of the protein that binds nucleotide and microtubules, joined to the neck and stalk of kinesin heavy chain (KHC) move toward microtubule plus ends, reversing the polarity of Ncd (2, 3). This finding raises several important questions about the kinesin motors. Foremost, can the Ncd stalk and neck change the direction of KHC movement? What are the determinants of motor directionality? Residues or regions of the protein must exist that contribute to or define the direction of motor movement. We examined the basis of kinesin motor polarity by constructing chimeric motors consisting of the Ncd stalk and neck joined to a KHC motor domain. The chimeric proteins were expressed in bacteria and assayed *in vitro* for directionality of movement on microtubules.

The design of the chimeric NcdKHC proteins analyzed in this study was guided by the crystal structures of the Ncd and KHC motor domains (4). The motor core (3, 5) refers to

the region of the motor domain conserved between Ncd and KHC, extending from the start of strand  $\beta$ 1 at the NH<sub>2</sub>-terminus to the end of helix  $\alpha$ 6 at the COOH-terminus (4) (Fig. 1). The neck of Ncd (residues 329 to 348) is defined as the region between the end of the predicted  $\alpha$ -helical coiled-coil stalk (6) and the start of the first conserved structural element, strand  $\beta$ 1, of the Ncd motor core (Fig. 1) (5). The neck of *Drosophila* KHC (residues 327 to 337) is defined as the region between the end of the last conserved structural element, helix  $\alpha$ 6, of the KHC motor core and the beginning of the predicted coiled-coil stalk (Fig. 1) (5). This definition of the KHC neck differs from those of others (7, 8), but it provides a working definition that can be tested experimentally.

We constructed six chimeric proteins for analysis, NcdKHC1–6 (Fig. 1) (9, 10) and tested lysates containing the induced chimeric proteins in microtubule gliding assays for their ability to bind microtubules to the cover slip surface and support microtubule gliding (11). All the chimeric proteins except NcdKHC3 showed this capability. NcdKHC3 bundled microtubules in solution but did not bind microtubules to the glass surface, which indicates that the region missing from the chimeric protein, the Ncd COOH-terminus, was needed for this function. The Ncd COOH-terminus was thus included in the other chimeric constructs analyzed in this study, except

NcdKHC6, in which the Ncd COOH-terminus was replaced by the KHC neck.

Polarity assays to determine directionality of motor movement on microtubules were carried out using axoneme-microtubule complexes consisting of a microtubule with a curved axoneme fragment at the minus end (12). NcdKHC1 showed minus-end-directed movement ( $n = 42$ ) (Fig. 2) with a velocity of  $1.4 \pm 0.18$   $\mu$ m/min (mean  $\pm$  SE;  $n = 26$ ) (Table 1). Controls with the same preparations of axoneme-microtubule complexes showed only minus-end movement for Ncd (GST-MC1) (13) and plus-end movement for kinesin. Thus, the Ncd stalk and neck reversed the polarity of movement of KHC. The gliding velocity of NcdKHC1 was about 10-fold slower than Ncd (Table 1).

In contrast to NcdKHC1, NcdKHC2 in polarity assays moved only toward microtubule plus ends ( $n = 10$ ) with a velocity of  $0.23 \pm 0.04$   $\mu$ m/min (mean  $\pm$  SE;  $n = 10$ ) (Table 1). Changing three amino acids in the neck of NcdKHC1 thus reversed the minus-end directionality of the motor and caused the mutant motor to move with the same polarity as KHC. A control with the same preparation of axoneme-microtubule complex showed only minus-end movement of Ncd (GST-MC1). The gliding velocity of NcdKHC2 was slow, >100-fold slower than kinesin and about 6-fold slower than NcdKHC1 (Table 1).

Like NcdKHC1, NcdKHC4 showed minus-end movement on microtubules ( $n = 23$ ) but with a velocity of  $0.57 \pm 0.08$   $\mu$ m/min (mean  $\pm$  SE;  $n = 11$ ) (Table 1). NcdKHC4 differs from NcdKHC1 by only a single amino acid residue, Leu<sup>345</sup> to Ala (L345A). The L345A mutation in the Ncd neck reduced motor velocity two- to threefold compared with NcdKHC1, but it did not alter the ability of the Ncd stalk and neck to reverse the polarity of KHC movement. In contrast to NcdKHC4, NcdKHC5 moved toward microtubule plus ends [ $n = 22$ ; velocity =  $0.23 \pm 0.04$   $\mu$ m/min (mean  $\pm$  SE;  $n = 9$ ) (Table 1)]. The two-residue shift alone at the neck-motor junction of NcdKHC5 thus reverted the minus-end movement of NcdKHC1 to plus-end movement.

Polarity assays of NcdKHC6 showed minus-end movement of the chimeric motor on

Department of Microbiology, Duke University Medical Center, Durham, NC 27710, USA.

\*To whom correspondence should be addressed. E-mail: endow@galactose.mc.duke.edu